Available online at www.sciencedirect.com

SCIENCE DIRECT

Biochimica et Biophysica Acta 1711 (2005) 183–196

BIOCHIMICA ET BIOPHYSICA ACTA
BBA

http://www.elsevier.com/locate/bba

Review

Sensitivity of the brain transcriptome to connexin ablation

Dumitru A. Iacobas*, Sanda Iacobas, Marcia Urban-Maldonado, David C. Spray

Department of Neuroscience, Albert Einstein College of Medicine, 1410 Pelham Parkway South, Kennedy Center, Room 915C, New York, NY 10461, United States

Received 29 July 2004; received in revised form 24 November 2004; accepted 2 December 2004
Available online 22 December 2004

Abstract

Extensive studies on mice with total or partial disruption of either connexin43 (Cx43) or connexin32 (Cx32) have detected only subtle changes in central nervous system structure, growth, development, or function. We have used high density cDNA arrays to analyze the regulation, control, and coordination of the abundances of 7446 distinct transcripts in four brains, each of Cx43 null (K43), Cx43 heterozygous (H43), and Cx32 null (K32) mice as compared to the brains of wildtype (W) mice. The use of multiple samples allowed the determination of the statistical significance of gene regulation. Significantly regulated genes encoded proteins of all functional categories, extending beyond those that might be expected to depend on junctional communication. Moreover, we found a high degree of similarity between genes regulated in the K43 and H43 brains and a remarkable overlap between gene regulation in brains of K43 and K32. The regulated genes in both K43 and H43 brains showed an outstanding inverse coordination with the levels of expression of Cx43 in W brain, indicating that the regulated genes are largely predictable from their co-variance with Cx43 in the wildtype samples. These findings lead to the hypothesis that connexin expression may represent a central node in the regulation of gene expression patterns in brain.

Keywords: Connexin43; Connexin32; Connexin43 null mouse; Connexin32 null mouse; Connexin43 heterozygous mouse; Gene expression

Contents

* Corresponding author. Tel.: +1 718 430 4138; fax: +1 718 430 8594.
E-mail address: diacobas@aecom.yu.edu (D.A. Iacobas).

0005-2736/$ - see front matter © 2004 Elsevier B.V. All rights reserved.
doi:10.1016/j.bbamem.2004.12.002

1. Introduction

More than half of the approximately twenty known mammalian connexins [1] are expressed in the nervous system either during development or in the mature brain [2–5]. The importance of the expression of these connexins has been assumed to be in the formation of gap junctions, thereby providing direct cytoplasmic continuity from one cell to another; such coupling mediates rapid impulse transmission between certain neurons and less rapid transmission of second messengers between the glia (see [6,7] for reviews). However, cDNA array studies of astrocytes cultured from connexin43 (Cx43) deficient mice have detected a large number of genes with altered expression, including those related to apoptosis and growth, as well as transcription factors expected to impact broadly on gene expression patterns [8,9]. In order to explore the impact of connexin expression on the expression of other genes, we have undertaken gene expression studies described below comparing brains of newborn wildtype mice with those lacking Cx32 or Cx43. These connexins were chosen for comparison because they are normally expressed in distinct glial elements of the brain.

2. Expression of Connexin32 and Connexin43 in the nervous system

Connexin32 (Cx32 or gap junction beta-1) is the primary component of hepatocyte gap junctions [10,11]. Moreover, Cx32 is a major gap junction component in the myelinating cells of the CNS (oligodendrocytes: [4,12,13]) and in the PNS (Schwann cells: [13–15]), where it is hypothesized to play the unusual role of providing a nutritional shunt from the outermost Schwann cell cytoplasm to the innermost, adaxonal regions [13,16,17]. Cx32 mutations are responsible for the X-linked form of Charcot-Marie-Tooth disease (CMTX), a progressively developing demyelinating peripheral neuropathy [14,18]. Cx32 knockout mice are viable through adulthood, and older animals are prone to slowed peripheral nerve conduction, analogous to the late onset of human CMTX disease [19,20].

Connexin43 (Cx43 or gap junction alpha-1) is the most widespread gap junction protein in mammals, where it occurs in almost every tissue [21,22]. Cx43 is a primary component of intercellular gap junction channels in cardiac tissue [23] and in astrocytes, the most abundant glial cell type in the brain [24–27]. In astrocytes, Cx43 gap junctions mediate ionic and metabolite exchange that contributes to potassium siphoning from around the active neurons and to long-range signaling (so-called “calcium waves”; see [7] for a review). Because Cx43 is distributed within the domains of single astrocytes, as well as between processes of neighboring astrocytes [28,29], it is likely that it forms autaptic contacts onto single astrocytes, somewhat analogous to the arrangement of Cx32 in Schwann cells. Cx43 also occurs between neural progenitors in early development [30–32]. Cx43 null mice die at birth due to a developmental cardiac abnormality, where hyperplasia blocks blood flow exiting from the right ventricular outflow tract to the lungs [33]; heterozygous Cx43(+/−) mice do not display this defect and are viable. Brains of Cx43 null mice are grossly normal [34], although the migration of neural progenitors is demonstrably altered compared to wildtype littermates when certain time points are critically examined [35]. Previous microarray studies have indicated that Cx43 expression is altered in both acute and chronic stages of multiple sclerosis [36] in Alzheimer disease [37], Huntington’s disease [38], and in other neural disorders [39,40].

3. Application of cDNA arrays to the analysis of gene expression in connexin null brains

3.1. cDNA microarrays

For the studies described here, we have used cDNA arrays produced at Albert Einstein College of Medicine. These arrays were co-hybridized with DNAs obtained by reverse transcription in the presence of fluorescent dUTPs (labeled with 532 nm emitting Cy3 or 635 nm emitting Cy5) of total RNA extracted from the tissues to be compared and a sample reference. Fluorescence signals of the co-hybridized arrays are then compared. As illustrated in Fig. 1A, a spot in the pseudo-color 8-bit image of the merged two 16-bit tiffs obtained by dual scanning of the hybridized array at 635 nm and 532 nm will appear yellow if that mRNA is similarly abundant in the two extracts or will be biased toward green or red if the abundance of mRNA is higher in one source or the other.

The arrays contain 27,571 spotted sequences: 15,693 spots probe 7455 distinct mouse genes encoding known protein products, 11,686 spots correspond to mouse ESTs whose annotation was incomplete at the date of the study (and thus eliminated from the expression analysis), and 192 spots contain bacterial sequences for quality control of the arrays.

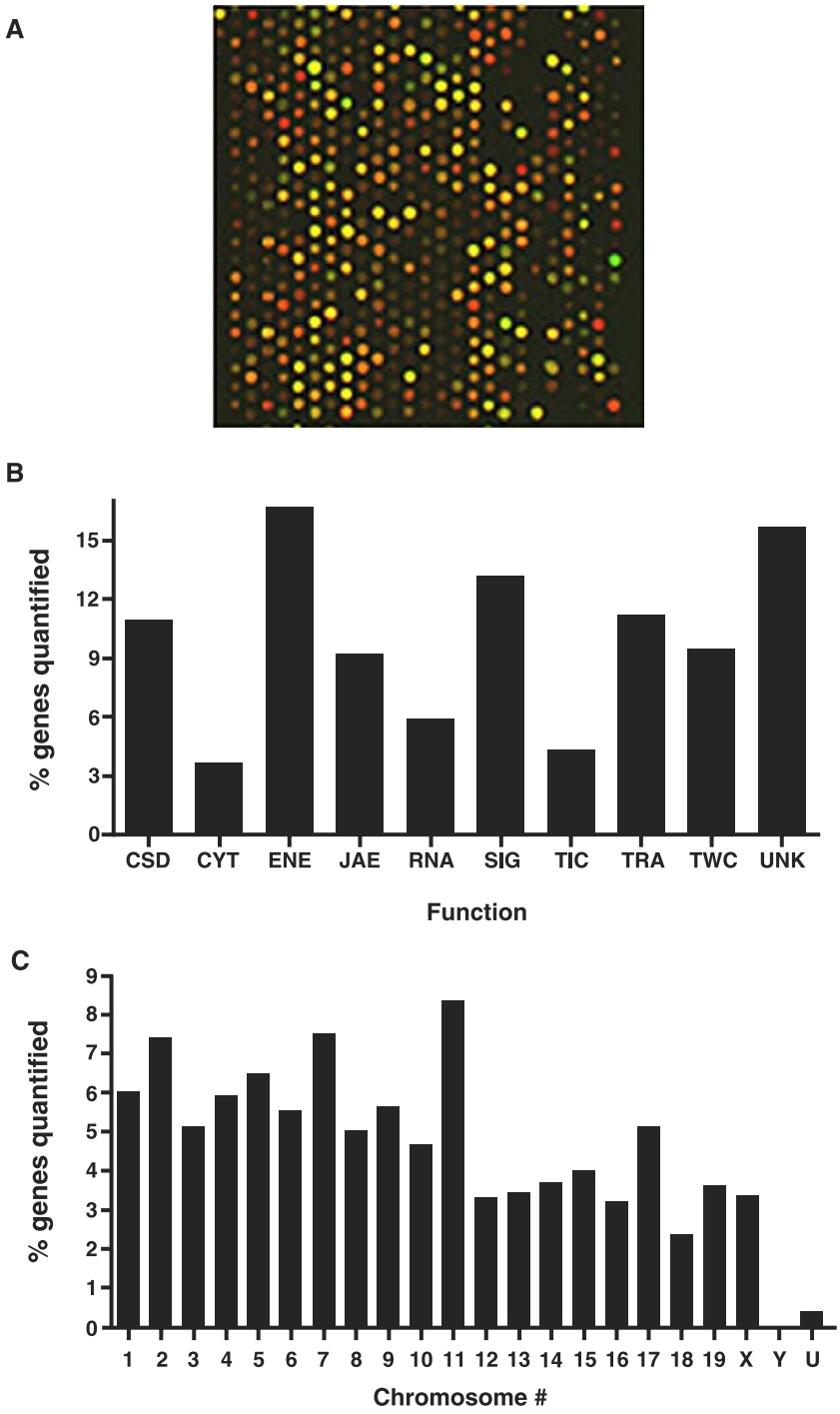

Fig. 1. The cDNA microarrays used in the study. (A) The 8-bit pseudo-color image of one of 48 blocks (23×26 spots) from a hybridized cDNA array hybridized with green-labeled wildtype brain extract and red-labeled reference. Red/green spot indicates a higher abundance of the probed transcript in the corresponding extract while a yellow spot indicates close abundances. (B) Functional classification of the 7446 adequately quantified genes with known protein products in the arrays used for this study. The functional classes were: CSD=cell-cycle–shape-differentiation–death, CYT=cytoskeleton; ENE=energy-methabolism, JAE=junction–adhesion–extracellular matrix; RNA=RNA processing; SIG=cell signaling; TIC=transport of small molecules and ions into the cells; TRA=transcription; TWC=transport of ions/molecules within the cells; UNK=function not yet assigned (see text for content and sub-categories). (C) Chromosomal location of the quantified genes. Note that no gene from chromosomes 20–22 was quantifiable on the array and only two quantifiable genes were located on chromosome Y. U=unknown chromosomal location.

Genes were categorized according the functions performed by their protein products in the following classes and subcategories (modified from [8]): CSD=cell cycle, shape, differentiation, death (A=apoptosis; C=cell cycle (cyclin); D=development, differentiation, organogenesis; G=growth factors, hormones, cytokines; S=shape; N=onco-

genes; O=others); CYT=cytoskeleton; ENE=energy metabolism (MIT=mitochondrial proteins involved in cyclic acid cycle, respiratory chain; L=lipid metabolism; D=degradation such as in peroxisomes, proteasome ubiquitination; G=glycolysis, glycogenesis; O=others); JAE=cell junction, adhesion, extracellular matrix (A=antigens, integrins; G=globulins and blood; M=extracellular matrix, laminin; J=junction and associated proteins; P=proteases (such as metalloproteinases); O=others); RNA=RNA processing (M=mRNA; R=rRNA; T=tRNA; MIT=Mitochondrial RNA); SIG=cell signaling (G-protein coupled receptors, PKA, PKC, cAMP, calcium, MAPK, SH2, SH3, and Ca-binding proteins); TIC=transport of small molecules and ions into the cells (transporters, ion channels, and ionotropic receptors); TRA=transcription (D=DNA transcription factors; P=DNA processing (such as polymerases); O=Others); TWC=transport of ions/molecules within the cells (vesicles, kinesin, endosomes, proteosomes, protein folding, lysosomes, and nuclear transport); UNK=function not yet assigned. As shown in Fig. 1B and C, the quantified distinct genes with known protein products belonged to all functional classes and were located on all chromosomes.

3.2. mRNA sources and array hybridization

All adult wildtype (used to prepare the sample composite RNA reference), neonatal wildtype (W), and connexin43 heterozygous (H43) mice [33] were from the C57BL/6j strain obtained from Jackson Laboratory (Bar Harbor, ME), while founders of our colony of connexin32 null (K32) C57BL/6j mice were provided by Dr. Klaus Willecke [41]. The mice were bred and maintained in our AAALAC-accredited animal facility, and genotypes of offspring from matings of H43 mice were determined by tail PCR [34,42]. The mice were decapitated under aseptic conditions, according to protocols approved by the AECOM Animal Use Committee, and organs were removed and immediately processed. The K43, H, and W mice described in this paper were obtained from the same two litters. A composite RNA was prepared as sample reference (R) for these studies in sufficient quantity for the entire projected experiment from selected amounts of total RNA extracted from ten adult mouse tissues (aorta, brain, heart, kidney, liver, lung, ovary/testicles, spleen, and stomach-equal amounts from males and females). This combination of source tissues provided a high diversity of genes expressed in the midrange of the detection system for the AECOM mouse cDNA microarrays.

60 μg total RNA, extracted in trizol (according the AECOM protocol, http://www.aecom.yu.edu/home/molgen/funcgenomic.html) from the composite reference R and from brains of each of the four W, K32, K43, or H43 mice, was reverse transcribed into cDNA using fluorescent dUTPs [Cy3-dUTP (green) and Cy5-dUTP (red)]. Each of the 16 green-labeled brain extracts (four brains from each of the four groups: W, K43, H43, and K32) and the red-labeled reference extracts were co-hybridized overnight at 50 °C with cDNA microarrays produced by the Microarray Facility of the Albert Einstein College of Medicine (http://www.microarray1k.aecom.yu.edu). Two other slides were used for the so-called "yellow test", in which red and green labeled R-extracts were hybridized against each other in order to validate the protocol and to estimate the technical noise, following the experimental design used in previous experiments [8]. These additional slides were scanned several times at different pairs of photomultiplier tube (PMT) voltages to determine the PMT settings that best balanced the recordings of the two channels of the scanner and accomplished an acceptable compromise between the numbers of spots eliminated because of low signal and those eliminated because of saturated pixels. After hybridization, the slides were washed at room temperature, using solutions containing 0.1% sodium dodecyl sulfate (SDS) and 1% SSC (3 M NaCl+0.3 M sodium citrate) to remove the non-hybridized cDNAs.

3.3. Experimental design and array scanning and normalization

For this study, we have used the reference sample strategy (RSS), in which the green-labeled specimens to be compared were co-hybridized with a red-labeled universal reference to avoid the non-uniform bias toward one label [43–48]. All microarrays were scanned with an Axon GenePix® 4000A scanner at the same PMT settings (750 V at 635 nm channel and 670 V at 532 nm channel) as determined in the "yellow test" and data were acquired through GenePix™ Pro 4.0 software (http://www.axon.com). The spots with substantial local imperfections (customarily flagged by the acquisition program), those for which the medians of the foreground signals (F) were not significantly ($P<0.001$) higher than the medians of the background signals (B) in both channels, and those with saturated pixels were eliminated from the analysis to avoid inadequate quantification.

The background-subtracted signals were normalized through an in-house developed iterative algorithm, alternating within-array normalization with inter-array normalization until the average corrected ratio differed by less than 5% from the previous one. The normalization reduced the average inter-array coefficient of variation, CV(R;s) (standard deviation/average value), of the background-subtracted fluorescence signal of each spot s of the red-labeled universal mouse reference in all 18 arrays from 32% to 15%, which is close to the 12% reported average CV in StaRT-PCR studies [49]. Since all arrays were obtained from the same spotting series and equal aliquots of red-labeled reference were hybridized with all arrays, this variability represents an estimate of the "technical noise" in printing, hybridizing, scanning, and gridding the arrays.

3.4. Methods of analysis: A. Identification of regulated genes and global characterization of altered expression pattern

The background-subtracted fluorescence signals of the brain transcripts normalized to the reference were averaged for all $n(j)$ valid spots probing the same gene j and the average normalized ratios (hereafter denoted by $\psi(j;W/R)$ or $\psi(j;G/R)$, where G=K43, H43, K32) of the transcript abundances in the studied specimens as compared to when the reference were used for further analysis. The detection of significantly regulated genes relied on both fold changes in expression ratio (which is limited by the technical noise of the method and expression variability among animals) and on the statistical significance of the two-tailed t-test for equality of two ratios [50] with a Bonferroni type adjustment [51,52] applied to the redundancy groups. Therefore, a gene j was considered significantly regulated in the genotype G as compared to the wildtype if and only if the following conditions imposed to the absolute expression ratio $|x(j;G/W)|$ (negative for down-regulation) and to the p-value $p(j;G/W)$ are satisfied:

$$|x(j;G/W)| \equiv \frac{\psi(j;G/R)}{\psi(j;W/R)} > \theta(j;G/W) \equiv \frac{1+\left|t\left(4n(j)-1;\frac{\alpha}{2}\right)\right| \times \frac{CV(G;j)}{\sqrt{4n(j)-1}}}{1-\left|t\left(4n(j)-1;\frac{\alpha}{2}\right)\right| \times \frac{CV(W;j)}{\sqrt{4n(j)-1}}} \quad (1)$$

$$p(j;G/W) \equiv \sum_{i=1}^{n(j)} \omega(i;j;G/W) < 0.05$$

where $\theta(G/W;j)$ is the threshold ratio; $CV(G;j)$ is the coefficient of variability of gene j in the genotype G=K43, H43, or K32; $t(4n(j)-1;\alpha/2)$ is the Student score for $4n(j)-1$ degrees of freedom and significance $\alpha/2$ (from the maximum error of estimate in the two-tailed test); and $\omega(i;j;G/W)$ is the p-value of the hybridization regulation of spot i probing gene j when the genotype G was compared to the wildtype.

The global alteration of the transcriptome induced by total or partial disruption of each connexin gene was quantified through the calculation of the redefined transcriptomic patholog [8,53,54] of genotype G with respect to the wildtype, $P(G,W)$:

$$P(G/W) = \frac{100}{U}\sqrt{\sum_{j=1}^{U}\left(\frac{x(j;G/W)}{\theta(j;G/W)} \times \frac{1-p(j;G/W)}{1-\pi(G/W)}\right)^2} \quad (2)$$

where U is the number of distinct genes that have been considered and $\pi(G/W)$ is the significance cut-off imposed for a gene to be considered as significantly regulated. In this study, we have used $\pi(G/W)$=0.05 for all altered genotypes. Higher values of the patholog indicate more profound alteration of the affected transcriptome with respect to the wildtype.

3.5. Methods of analysis: B. Variability, control, and coordination of transcripts abundances

Compared to our previous paper [8], the α-significant Relative Estimated Variability (REV) of transcript j abundance in the genotype Γ (=W, K43, K32, H43) was redefined to eliminate the contribution of technical variability:

$$\mathrm{REV}(\Gamma;j) = \left(\sqrt{\frac{n(j)-1/4}{\chi^2(4n(j)-1;1-\alpha/2)}} + \sqrt{\frac{n(j)-1/4}{\chi^2(4n(j)-1;\alpha/2)}}\right)\left(\frac{s(\Gamma;j)}{\psi(j;\Gamma/R)} - CV(R;j)\right) \quad (3)$$

where $s(\Gamma;j)$ is the standard deviation and χ^2 is the chi-square score for $4n(j)-1$ degrees of freedom and $1-\alpha/2$ or $\alpha/2$ probabilities. In this study, we used α=0.05.

REV values were used to identify the most stably and unstably expressed genes in each genotype, to evaluate the control stringency of the transcript abundance (with high REV values meaning low control), to determine the change of control stringency induced by the total or partial disruption of Cx43 or Cx32, and to assign statistical significance to expression regulation.

The Gene Expression Stability [8] was used to categorize the genes as: exceptionally stably expressed (GES >99), very stably expressed (99≥GES>95), stably expressed (95≥GES>75), moderately stably expressed (75≥GES>50), moderately unstably expressed (50≥GES>25), unstably expressed (25≥GES>5), very unstably expressed (5≥GES>1), and exceptionally unstably expressed (GES ≤1). This classification was used to identify those genes with major changes in expression stability induced by total or partial connexin deletion.

Pearson's correlation coefficients between the normalized ψ-ratios were used to determine the expression coordination of two genes. In our case of four replicas, the 5% cut off values are: $0.9<\rho\leq 1$ for synergistic expression (abundances of transcripts of paired genes increased and decreased together from animal to animal), $-0.9<\rho\leq -1$ for antagonistic expression (inverse relationship of transcript abundances), and $|\rho|<0.05$ for independent expression (variations of expression levels of the two genes are not connected). Moderate correlations ($0.05\geq|\rho|\geq 0.9$) were eliminated from the analysis.

4. Gene expression in Cx43 null and heterozygous and Cx32 null brains

The study was performed according to the standards of Microarray Gene Expression Data Society (MGED), and data

complying with the "Minimum Information About Microarray Experiments" (MIAME) have been deposited in the National Center for Biotechnology Information (NCBI) Gene Expression Omnibus (GEO) database (http://www.ncbi.nlm.nih.gov/geo, platform GPL1698, series GSE1954, samples GSM34855 and 34858–34872).The main features and representative examples are considered below. 7446 distinct genes with known protein products were adequately quantified in all arrays used in this experiment. Seven genes with no valid spot in all arrays and two genes with significantly divergent results within their redundancy groups were eliminated from the analysis.

4.1. "*Normal*" and "*altered*" variability of transcript abundance

In order to statistically compare individual gene transcription levels in different samples, it is necessary to determine the extent to which expression varies within each sample population. For each of the adequately quantified genes in every set of four microarrays, we have calculated the Relative Estimated Variability (REV) of the transcript abundance. Fig. 2 presents the histograms of the REV values of all adequately quantified genes in brains from all genotypes.

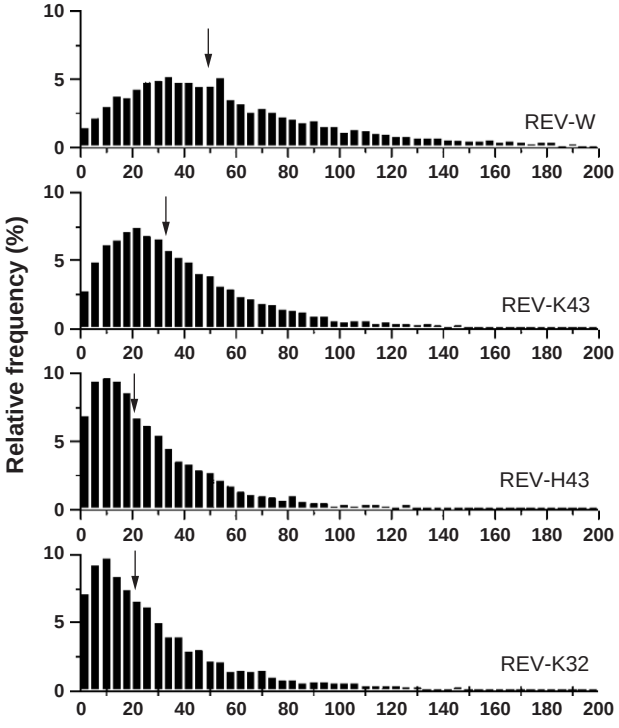

Fig. 2. Relative Estimated Variability (REV) of transcript abundance within sets of four brains from neonatal wildtype (W), Cx43 null (K43), and Cx43 heterozygous (H43) mice. The arrows indicate the median values. Note that the wildtype brain has the highest average REV and that the Cx43 heterozygous brains have lower average REVs than does the corresponding knock-out. Lower REV indicates higher stability, while higher REV indicates less stability.

Note that individual genes exhibited a wide range of REV values, indicating that expression variability is much higher for some genes than for others. The median REV value for neonatal wildtype brain was 49.7%. Remarkably, the distribution of REV values in brains with altered expression of connexins exhibited significantly lower median values: 32.2% (K43), 21.3% (H43), and 22.7% in K32. Since both connexin43 null and wildtype mice came from the same litters delivered by two H43 females, the reduced expression variability in K43 indicates the increased control of gene transcription presumably acting to compensate and limit the effects of deleting Cx43.

A list of the 21 most stably (GES >99) and 21 most unstably (GES <1) transcribed genes in the brains of neonatal wildtype mice is presented in Table 1. For each gene, GES values are also shown for each of the genetically manipulated brains to compare their stabilities with those of the wildtype. Note that deletion of one or both copies of Cx43 had different effects on the expression stability of individual genes. For example, the stability or instability of Mrps16, Rock2, Tuba4, and Ptbp1 was not essentially modified in the K43 brain compared to that of wildtype, and the stability or instability of Thoc1, Phf13, and Syngr2 in H43 were quite similar to that of the wildtype. The stability of genes such as Adcyap1r1, Elp3, Stmn4, and Ube2g1 was dramatically changed in the K43 brain but was less affected in the H43 brains. Thus, the modifications in gene expression stability resulting from the total (or partial) deletion of only one gene (Cx43 or Cx32) extended toward all functional classes. This finding suggests that the normal expression of connexins broadly influences the transcriptional control of other genes.

The sets of GES values in all three genetically manipulated brains were independent (correl(W-K43)=0.10, correl(W-H43)=0.02, correl(W-K32)=−0.00) when compared to the corresponding set in W brains, suggesting an independent alteration of the transcription control mechanisms of individual genes when the expression of Cx43 or Cx32 is disrupted. However, when the stability analysis in Cx43 null brains was restricted to the genes that were coordinately expressed with Cx43 in W brains, we found that expression stability increased for 67% of the genes synergistically expressed with connexin43 and decreased for 66% of the antagonistically expressed ones, indicating a tendency of expression stability change to follow the coordination degree.

4.2. Altered gene expression in Cx43 null and heterozygous and Cx32 null brains

Although only Cx43 or Cx32 was disrupted by homologous recombination, other genes that were significantly up- or down-regulated in the brains of these animals extended to all functional classes and all chromosomes, suggesting a high degree of complexity of the inter-gene relationships.

Table 1
Examples of most stably (high GES) and unstably (low GES) expressed genes in the brains of neonatal wildtype (W) mice and their stabilities in the brains of neonatal Cx43 null (K43), Cx43 heterozygous (H43), and connexin32 null (K32) mice

Name	Symbol	CHR	Func-C	W	K43	H43	K32	GES
A kinase (PRKA) anchor protein (gravin) 12	Akap12	7	SIG					
Adenylate cyclase activating polypeptide 1 receptor 1	Adcyap1r1	6	SIG					
Beta-1, 3-glucuronyltransferase 2 (glucuronosyltransferase S)	B3gat2	1	ENE-O					99 - 100
Bromodomain adjacent to zinc finger domain, 2A	Baz2a	10	TWC					
Calbindin-28K	Calb1	4	SIG					
Cleavage and polyadenylation specific factor 5	Cpsf5	8	RNA-M					
Elongation protein 3 homolog (S. cerevisiae)	Elp3	14	ENE-O					
Intracellular membrane-associated calcium-independent phospholipase A2 gamma	Ipla2(gamma) pending	12	ENE-L					95 - 99
Mitochondrial ribosomal protein S16	Mrps16	14	RNA-MIT					
Nuclear, casein kinase and cyclin-dependent kinase substrate	Nucks-pending	1	SIG					
Paired basic amino acid cleaving system 4	Pace4	7	RNA-M					
PHD finger protein 13	Phf13	4	UNK					
Protein tyrosine phosphatase 4a2	Ptp4a2	4	SIG					75 - 95
Purine rich element binding protein A	Pura	18	TRA-D					
Rho-associated coiled-coil forming kinase 2	Rock2	12	SIG					
Ribonuclease H1	Rnaseh1	12	RNA-M					
Sortilin 1	Sort1	3	TWC					
Steroid sensitive gene 1	Ssg1-pending	16	UNK					50 - 75
THO complex 1	Thoc1	18	CSD-A					
Transient receptor potential cation channel, subfamily M, member 7	Trpm7	2	TIC					
Tweety homolog 2 (Drosophila)	Ttyh2	11	UNK					
ATP-binding cassette, sub-family A (ABC1), member 2	Abca2	2	TIC					
Calcium channel, voltage-dependent, gamma subunit 4	Cacng4	11	TIC					25 - 50
Catenin beta	Catnb	9	JAE-J					
FXYD domain-containing ion transport regulator 2	Fxyd2	9	TIC					
Glucocorticoid induced transcript 1	Glcci1	6	SIG					
Guanine nucleotide binding protein (G protein), gamma 4 subunit	Gng4	13	SIG					
Jagged 2	Jag2	12	SIG					5 - 25
Myotrophin	Mtpn	6	CYT					
Open reading frame 61	ORF61	10	UNK					
Polypyrimidine tract binding protein 1	Ptbp1	10	UNK					
SRY-box containing gene 3	Sox3	X	TRA-D					
Stathmin-like 4	Stmn4	14	TWC					1 - 5
Synaptogyrin 2	Syngr2	11	TWC					
Syntaphilin	Snph	2	TWC					
Tubulin, alpha 4	Tuba4	1	CYT					
Ubiquitin-conjugating enzyme E2G 1 (UBC7 homolog, C. elegans)	Ube2g1	11	ENE-D					
UDP-Gal:betaGlcNAc beta 1, 4-galactosyltransferase, polypeptide 6	B4galt6	18	ENE-O					0 - 1
UDP-N-acetyl-alpha-D-galactosamine:polypeptide N-acetylgalactosaminyltransferase 9	Galnt9	11	ENE-O					
Vacuolar protein sorting 52 (yeast)	Vps52	17	TWC					
Xylosyltransferase II	Xylt2	11	ENE-O					
Zinc finger protein 318	Zfp318	17	UNK					

CHR=chromosomal location, FUNC-C=functional class. Note the stability change in brains with altered expression of connexins as compared to the corresponding wildtype ones. GES boxes were color-coded to help visual inspection of stability class. The GenBank Accession Number of the sequence is not presented because most results have been obtained by averaging the normalized net fluorescence signals of several spots probing the same gene.

Compared to wildtype brain, we found that 642 (8.6%) of the 7446 adequately quantifiable distinct genes with known protein products were significantly down-regulated in the K43 brain and 383 (5.2%) significantly up-regulated. The numbers of regulated genes were lower in the case of H43 brains, 347 (4.6%) down and 236 (3.2%) up, whereas in the K32 brains, 441 (5.9%) were down-regulated and 431 (5.8%) were up-regulated. Fig. 3 presents the distributions of the significantly regulated genes in functional classes for the three types of brains in which the expression of Cx43 or Cx32 was altered. The most striking common characteristic of the expression patterns in the brains of all three genotypes is the significant down-regulation of the genes in the CYT, ENE, and RNA classes.

Fig. 4 presents the similarities and dissimilarities in gene expression regulation in H43 and K32 brains as compared to that in K43. Remarkably, 58.7% of the significantly regulated genes in K32 were similarly regulated in K43 and only 0.2% oppositely regulated. When the analysis is restricted to genes significantly regulated in both knockouts, the similarly regulated genes represent 99.6% in both comparisons. When K43 and H43 brains were compared,

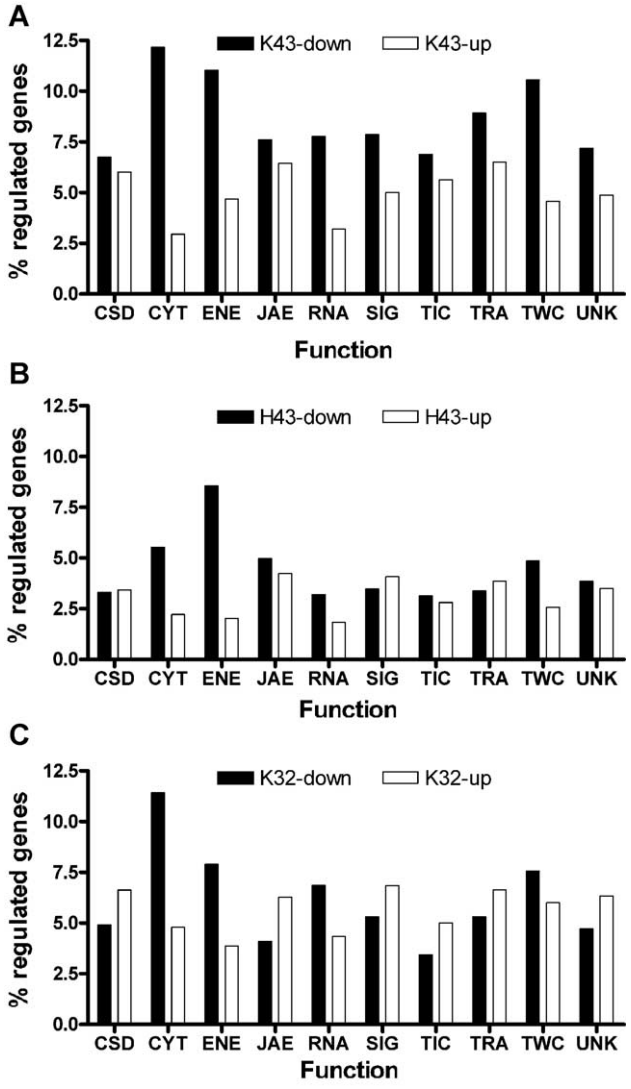

Fig. 3. Percentage of significantly regulated out of quantified genes within each functional class in brain of connexin deficient mice as compared to wildtypes. Note the overall down-regulation in K43 and the balance between down- and up-regulation in K32, as well as the predominance of down-regulated with respect to up-regulated genes in all three genotypes for CYT, ENE, and RNA genes.

44% of the significantly regulated genes in K43 were similarly regulated in H43 and only 0.2% were oppositely regulated, while 81.5% of the significantly regulated genes in H43 were similarly regulated in K43.

Table 2 presents examples of genes that were found to be significantly regulated in the brains of all genetically manipulated mice used in this study. The complete list can be found in Supplementary Table 1. 300 genes were significantly regulated in all genetically modified brains: 199 down-regulated and 101 up-regulated. Remarkably, each of these 300 genes was regulated in the same direction in all three types of brains.

It is noteworthy that several similarly regulated genes in all three types of brains with altered expression of Cx43 or Cx32 are directly involved in brain development (e.g. the up-regulated Emx2=empty spiracles homolog 2 (*Drosophila*) and Hhex=hematopoietically expressed homeobox and the down-regulated Napa=*N*-ethylmaleimide sensitive fusion protein attachment protein alpha), transcription regulation (e.g. Nfib=nuclear factor I/B; Atb1=AT motif binding factor 1; Trp53bp1=transformation related protein 53 binding protein 1), or signaling mechanisms (e.g. Lcp2=lymphocyte cytosolic protein 2; Socs5=suppressor of cytokine signaling 5; Rgs2=regulator of G-protein signaling 2; Gnaj2=guanine nucleotide binding protein, alpha inhibiting 2).

The calculation of the transcriptomic patholog allows a quantitative overall assessment of the degree of alteration in gene expression in each genotype. The values of the transcriptomic patholog were 1.49 for K43, 1.39 for H43, and 1.80 for K32. Thus, the brain transcriptome is more substantially altered when totally deleting Cx32 than Cx43, even though the number of regulated genes was smaller in K32. The alteration in the heterozygous brain is smaller than in K43, but it is significantly higher than half the value of the transcriptomic patholog for the total knock-out. The overall gene expression alteration in H43 is thus more extensive than expected from a simple dependence on Cx43 gene dosage.

4.3. Coordinated expression with Cx43 in wildtype predicts expression regulation in Cx43 null and heterozygous brain

For each individual gene that was significantly above background on each of the four arrays, we determined in wildtype brains whether expression was synergistically ($\rho>0.9$), antagonistically ($\rho<-0.9$), or independently ($|\rho|<0.05$) expressed with that of Cx43. We found 397 genes synergistically expressed with Cx43, 373 antagonis-

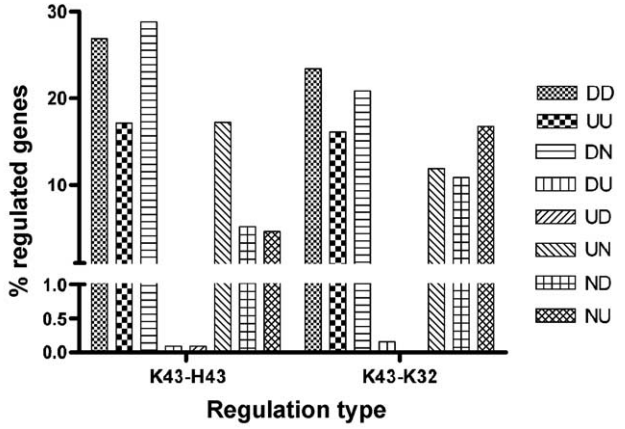

Fig. 4. Similarities and dissimilarities in gene expression regulation. DD=down-regulated in both types of connexin altered brains; UU=up-regulated in both DU; UD=opposite regulations DN, ND, UN; NU=down-/up-regulated in one brain and not-regulated in the other. Note the negligible opposite regulations, the remarkable similarity between the regulations in the two knockouts, and the 81.5% [=(DD+UU)/(DD+UU+NU+ND)] inclusion of the regulated part of the H43 transcriptome in the regulated part of the K43 transcriptome.

Table 2
Examples of genes with similar regulation in K43, H43, and K32 brains

Name	Symbol	CHR	FUNC-C	X-K43	P-K43	X-K32	P-K32	X-H43	P-H43
Annexin A2	Anxa2	9	SIG	−2.05	0.048	−2.47	0.000	−2.04	0.000
ATPase, H+transporting, V0 subunit D isoform 1	Atp6v0d1	8	TIC	−2.64	0.005	−3.13	0.003	−2.57	0.005
ATP-binding cassette, sub-family G (WHITE), member 4	Abcg4	9	TIC	−2.60	0.006	−2.24	0.001	−2.56	0.000
Cathepsin D	Ctsd	7	JAE-P	−2.22	0.003	−2.48	0.003	−2.16	0.004
Chromodomain helicase DNA binding protein 1	Chd1	17	TRA-P	−3.11	0.012	−1.93	0.000	−2.60	0.000
Coated vesicle membrane protein	Rnp24-penc	5	TWC	−2.32	0.012	−2.70	0.001	−2.05	0.005
Ephrin B2	Efnb2	8	JAE-J	−3.09	0.003	−2.92	0.003	−2.72	0.004
Eukaryotic translation initiation factor 2, subunit 3, structural gene X-linked	Eif2s3x	X	RNA-M	−2.43	0.004	−2.64	0.001	−2.23	0.005
Methionine adenosyltransferase II, alpha	Mat2a	6	ENE-O	−2.09	0.040	−1.99	0.002	−2.08	0.005
Nuclear factor I/X	Nfix	8	TRA-D	−3.42	0.006	−3.27	0.003	−3.34	0.004
Ornithine decarboxylase antizyme	Oaz1	10	ENE-O	−2.36	0.023	−2.20	0.003	−2.01	0.005
Oxoglutarate dehydrogenase (lipoamide)	Ogdh	11	ENE-MIT	−3.48	0.040	−3.29	0.000	−3.31	0.000
Peroxiredoxin 6	Prdx6	1	ENE-D	−2.64	0.016	−3.29	0.002	−2.44	0.010
Phosphoribosyl pyrophosphate synthetase 1	Prps1	X	ENE-O	−2.81	0.002	−2.44	0.001	−2.53	0.001
Platelet derived growth factor, alpha	Pdgfa	5	CSD-G	−3.03	0.003	−3.49	0.001	−2.97	0.001
Polymerase delta interacting protein 38	Pdip38-penc	11	TRA-P	−2.47	0.040	−2.22	0.001	−2.11	0.001
Procollagen-lysine, 2-oxoglutarate 5-dioxygenase 3	Plod3	5	ENE-O	−3.33	0.009	−3.25	0.008	−3.11	0.007
Proteasome (prosome, macropain) 26S subunit, non-ATPase, 13	Psmd13	7	ENE-D	−3.76	0.040	−3.28	0.000	−3.11	0.000
RAB28, member RAS oncogene family	Rab28	5	CSD-N	−2.12	0.040	−1.84	0.008	−2.09	0.004
Retinoblastoma binding protein 6	Rbbp6	7	TRA-D	−3.54	0.040	−4.01	0.000	−3.27	0.000
Trans-golgi network protein	Tgoln1	6	TWC	−2.02	0.010	−3.74	0.000	−2.01	0.003
Wolf-Hirschhorn syndrome candidate 2 homolog (human)	Whsc2h	5	UNK	−2.54	0.003	−2.42	0.003	−2.13	0.008
Abelson helper integration site	Ahi1	10	UNK	6.04	0.008	6.66	0.007	7.78	0.001
BH3 interacting domain death agonist	Bid	6	CSD-A	2.02	0.007	2.35	0.000	2.14	0.001
Copine 1	Cpne1	2	SIG	1.97	0.005	1.95	0.004	2.39	0.004
Cyclin M4	Cnnm4	1	CSD-C	3.35	0.005	2.84	0.002	3.02	0.004
DEAH (Asp-Glu-Ala-His) box polypeptide 8	Dhx8	11	TRA-P	2.08	0.040	3.44	0.002	4.11	0.007
Drebrin 1	Dbn1	13	CYT	2.33	0.017	2.93	0.004	2.90	0.006
F-box only protein 21	Fbxo21	5	ENE-D	2.15	0.045	2.54	0.001	2.48	0.003
Glucocorticoid induced gene 1	Gig1-pendir	3	UNK	2.93	0.050	9.72	0.004	5.39	0.006
H19 fetal liver mRNA	H19	7	RNA-M	2.54	0.017	2.68	0.002	3.41	0.000
Kinesin family member 1A	Kif1a	1	TWC	2.96	0.041	7.54	0.001	6.55	0.000
Myeloid/lymphoid or mixed-lineage leukemia	Mll	9	UNK	2.56	0.010	2.02	0.005	3.48	0.000
Neuronal d4 domain family member	Neud4	7	TRA-D	2.36	0.020	2.76	0.001	3.55	0.000
Oligophrenin 1	Ophn1	X	SIG	2.04	0.040	2.20	0.004	4.57	0.000
Plexin A4	Pixna4	6	JAE-J	3.07	0.035	5.44	0.007	4.49	0.009
Protocadherin gamma subfamily C, 4	Pcdhgc4	18	JAE-J	2.28	0.018	4.10	0.000	3.62	0.009
SH3 domain binding glutamic acid-rich protein-like 3	Sh3bgr13	4	UNK	2.25	0.008	2.71	0.002	3.06	0.000
SWI/SNF related, matrix associated, actin dependent regulator of chromati	Smarca4	9	TRA-D	2.47	0.015	3.38	0.002	3.57	0.001
Transformation related protein 53 binding protein 1	Trp53bp1	2	TRA-D	2.16	0.005	2.67	0.000	3.31	0.000
Transient receptor potential cation channel, subfamily V, member 2	Trpv2	11	TIC	2.30	0.035	2.57	0.005	2.10	0.007
UDP-Gal: betaGlcNAc beta 1, 3-galactosyltransferase, polypeptide 2	B3galt2	1	ENE-O	2.05	0.010	2.37	0.000	2.52	0.001
V-abl Abelson murine leukemia oncogene 1	Abl1	2	CSD-N	2.00	0.019	3.36	0.000	3.18	0.001

CHR=chromosomal location, FUNC-C=functional class, X-genotype=expression ratio of the indicated genotype (e.g. K43) with respect to wildtype brains, P-genotype=*p*-value.

tically expressed, and 88 independently expressed. Fig. 5 presents the distribution among functional classes of the genes that were coordinately expressed with Cx43 in the W brain. On average, 11% of the genes within each functional class were found to be coordinately expressed with Cx43, consistent with high numbers of genes significantly regulated by Cx43 deletion.

Within the set of genes that were synergistically and antagonistically expressed with Cx43 in the wildtype brain and that were also significantly regulated in Cx43 null and heterozygous brains, the type of significant regulation was correctly predicted for 169 (91.8%) genes in K43 and for 80 (84.2%) in H43 compared to 15 falsely predicted in both K43 and H43 brains. Table 3 presents some examples of genes that were synergistically or antagonistically expressed with Cx43 in wildtype brains and whose significant down-/up-regulation was accurately predicted in both K43 and H43 brains.

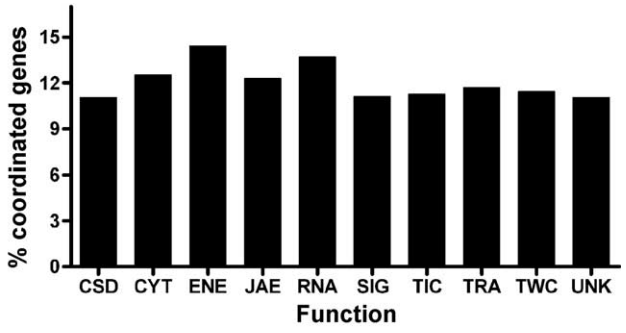

Fig. 5. Distribution in functional classes of the coordinately expressed genes with Cx43 in the brain of neonatal wildtype mouse. The values represent the percentages of quantified genes in each class that were found significantly ($P<0.05$) coordinately (i.e. synergistically or antagonistically) expressed with Cx43. Compared to the irregular abundance of functional classes within the population of quantified genes, the relatively uniform percentage of genes coordinately expressed with Cx43 in functional classes suggests that the gene encoding Cx43 is a node in transcriptional control of genes expressed in brain.

Note from both Table 3 and Fig. 5 that the genes coordinately expressed with Cx43 belong to all functional categories and are located on all chromosomes, again indicating the high degree of complexity of gene expression regulation.

5. Unanswered question: are connexin genes "nodes" in transcriptional control?

There is a conceptual difference between examining the hypothesis that the expression of a few selected genes is altered in connexin null brains using techniques such as Northern or Western blots and the screen of thousands genes at a time performed in microarray studies. The unbiased nature of the high throughput screen leads to abundant testable hypotheses regarding biological correlates. In order to facilitate such further studies, we have classified the genes according to functions of their proteins and included this classification in all tables, enabling other investigators to identify and verify individual pathways that are altered in the Cx null mice, as we are doing ourselves in follow-up studies.

Our study revealed that transcriptomic changes induced in the brain by the disruption of one or both copies of the genes encoding connexin43 or the deletion of connexin32 extended to genes belonging to all functional classes and located on all chromosomes. This finding is consistent with our previous study using cDNA arrays to compare wildtype and Cx43 null astrocytes in culture [8,9] and wildtype and Cx43 null mouse hearts [67]. In the astrocyte study, we noted the numerous alterations in genes encoding proteins involved in apoptosis, cell cycle, and growth. We hypothesized that the altered expression of these genes rather than the changes in intercellular coupling in the Cx43 null astrocytes might be responsible for their altered growth rate and sensitivity to apoptotic stimuli. Phenotypic alterations reported in Cx43 null brains include slight changes in progenitor cell migration at certain developmental timepoints [35], increased sensitivity to ischemia [55], and enhanced spreading depression [56]. Mutations in Cx43 underlie oculodentodigital dysplasia, with symptoms including developmental malformation and frequent neurological symptoms [57]. For Cx32 null brains, increased vulnerability to ischemia [58] and neuronal hyperexcitability and myelination defects have been reported [59]. Not all CMTX patients with coding region Cx32 mutations exhibit CNS abnormalities [60], but there are reports of white matter lesions [61], transient white matter abnormalities after returning from high altitude [62], retarded central conduction velocity [63,64], and other abnormalities [65].

It has generally been assumed that phenotypic differences in connexin null mice were attributable to the loss or dysfunction of intercellular channels normally formed by the missing gap junction protein. Alternatively, however, altered phenotypes might arise from altered expression of genes that are coordinately expressed with connexins. The present study indicates that such coordinated expression with Cx43 exists in the brain transcriptome and raises the hypothesis that diseases in which connexin expression is altered may result in effects on other genes similar to the patterns detected here.

We have found a remarkable overlap between the transcriptomic effects of disrupting Cx43 and Cx32 in brain, although each connexin deletion produced more significant differences than identities. This finding is consistent with studies characterizing transgenic animals in which one connexin was substituted for another. In those so-called knockin-knockout studies [66], it was concluded that connexins possess both unique as well as shared functions.

As noted in Section 2, Cx43 null mice die at birth due to outflow tract obstruction. Thus, changes detected in neural gene expression patterns might reflect, in part, the cardiovascular consequences of connexin43 deletion, leading to the death of Cx43 null mouse as a neonate. However, H43 mice are phenotypically normal, and the 81.5% inclusion of the regulated part of the H43 transcriptome in the regulated part of the K43 transcriptome suggests that most of the changes in gene expression reflect the impact of Cx43 deletion rather than secondary pathology. Moreover, as discussed below, the substantial overlap between genes regulated in K43 and those coordinately expressed with Cx43 in the wildtype suggest that the deletion mutant exaggerates the normally occurring covariance between the expression of Cx43 and other genes.

By determining the Relative Estimated Variability (REV) of transcript abundances, we found both exceptionally stably and exceptionally unstably expressed genes in all genotypes. Since the basic expression mechanisms should be the same in all animals from an experimental set, this diversity of expression stability can be interpreted as differential sensitivity to local conditions, leading to the conclusion that

Table 3
Examples of regulated genes in both Cx43 null (K43) and heterozygous (H43) brains whose type of regulation was accurately predicted by the expression coordination (COR) with Cx43 in wildtype brain

Name	Symbol	CHR	FUNC-C	COR	X-K43	P-K43	X-H43	P-H43
Hemopexin	Hpxn	7	TIC	0.96	−7.48	0.015	−9.58	0.009
Selenoprotein P, plasma, 1	Sepp1	15	UNK	0.91	−4.64	0.009	−3.65	0.009
Inhibitor of DNA binding 2	Idb2	12	TRA-D	0.94	−4.63	0.039	−4.74	0.009
Purine rich element binding protein B	Purb	11	TRA-D	0.95	−4.53	0.024	−5.46	0.009
Solute carrier family 25, member 5	Slc25a5	X	TWC	0.92	−4.07	0.019	−5.03	0.006
Glutathione *S*-transferase, pi 2	Gstp2	19	ENE-O	0.93	−3.42	0.008	−3.77	0.002
Platelet derived growth factor, alpha	Pdgfa	5	CSD-G	1.00	−3.03	0.003	−2.97	0.001
Gelsolin	Gsn	2	CYT	0.98	−2.60	0.016	−2.82	0.001
Fibrinogen, alpha polypeptide	Fga	3	JAE-M	0.98	−2.47	0.019	−5.13	0.000
Proteolipid protein (myelin)	Plp	X	JAE-J	0.91	−2.36	0.032	−5.64	0.000
Ectonucleotide pyrophosphatase/phosphodiesterase 5	Enpp5	17	ENE-D	0.90	−2.25	0.026	−2.64	0.009
Growth hormone inducible transmembrane protein	Ghitm	14	UNK	0.99	−2.20	0.009	−2.74	0.000
Staufen (RNA binding protein) homolog 1 (*Drosophila*)	Stau1	2	RNA-M	0.95	−2.11	0.030	−2.62	0.005
Integrin linked kinase	Ilk	7	JAE-A	0.96	−2.10	0.023	−3.01	0.000
Peroxiredoxin 4	Prdx4	X	ENE-D	0.94	−2.05	0.012	−2.10	0.005
FK506 binding protein 1a	Fkbp1a	2	ENE-O	0.95	−2.05	0.031	−2.38	0.004
Dishevelled associated activator or morphogenesis 2	Daam2	17	TRA-D	1.00	−1.97	0.007	−3.36	0.000
Pyruvate dehydrogenase (lipoamide) beta	Pdhb	14	ENE-G	0.90	−1.95	0.007	−2.11	0.004
Syndecan 2	Sdc2	15	CYT	0.96	−1.86	0.009	−2.19	0.001
Adenylosuccinate synthetase 2, non muscle	Adss2	1	ENE-D	1.00	−1.81	0.037	−2.03	0.007
Prostaglandin E receptor 4 (subtype EP4)	Ptger4	15	SIG	−0.91	1.61	0.029	2.05	0.004
Seryl-aminoacyl-tRNA synthetase 1	Sars1	3	ENE-O	−0.92	1.62	0.019	2.08	0.005
Caspase 9	Casp9	4	CSDA-A	−0.93	1.62	0.028	2.09	0.003
Ftsj homolog (*E. coli*)	Ftsj	X	UNK	−0.91	1.63	0.006	2.09	0.002
Glutamate receptor, ionotropic, kainate 3	Grik3	4	TIC	−0.94	1.64	0.024	3.43	0.009
Transforming growth factor, beta 2	Tgfb2	1	CSD-G	−0.93	1.64	0.029	2.24	0.002
Hepatocyte growth factor	Hgf	5	CSD-G	−0.92	1.65	0.021	3.11	0.009
Plexin B3	Plxnb3	X	JAE-J	−0.93	1.68	0.015	2.28	0.001
Thyrotropin releasing hormone	Trh	6	CSD-G	−0.97	1.71	0.017	2.03	0.001
Ribosomal protein S26	Rps26	10	RNA-M	−0.92	1.74	0.005	2.06	0.010
Acetylcholinesterase	Ache	5	ENE-O	−0.95	1.76	0.006	2.08	0.004
Neural-salient serine/arginine-rich	Nssr	4	UNK	−0.96	1.79	0.017	2.08	0.009
RecQ protein-like 5	Recql5	11	UNK	−0.91	1.79	0.032	2.29	0.008
Heat shock protein 4	Hspa4	11	TWC	−0.90	1.84	0.013	2.37	0.004
AT motif binding factor 1	Atbf1	8	TRA-D	−0.98	1.92	0.030	2.17	0.002
V-abl Abelson murine leukemia oncogene 1	Abl1	2	CSD-N	−0.90	2.00	0.019	3.18	0.001
Neoronal d4 domain family member	Neud4	7	TRA-D	−0.96	2.36	0.020	3.55	0.000
Growth factor receptor bound protein 2	Grb2	11	TWC	−0.92	2.46	0.023	2.03	0.009
Myeloid/lymphoid or mixed-lineage leukemia	Mll	9	UNK	−0.97	2.56	0.010	3.48	0.000
Cyclin M4	Cnnm4	1	CSD-C	−0.93	3.35	0.005	3.02	0.004

X-genotype=expression ratio, P-genotype=*p*-value. Note that synergistically (COR >0.9) expressed genes with Cx43 in wildtype were down-regulated in K43 and H43 and that antagonistically (COR <−0.9) expressed genes with Cx43 in wildtype were up-regulated in K43 and H43. Observe that the coordinately expressed genes belong to all functional classes and are located in all chromosomes represented on the array.

the stringency of the control of the transcript abundance is different among genes. We expect that the exceptionally tightly controlled genes may be critical for cell survival and/or phenotypic expression, while those with very relaxed control may allow adaptation to continuously changing environmental conditions. In addition, this analysis revealed that even for genes whose expression level was not significantly regulated in brains of mice with connexin deficiencies, the stringency of the transcript abundance control was regulated, again illustrating the complexity of transcriptomic response to ablation of a single gene.

Remarkably, both total and partial disruption of Cx43 diminished the median REV. Since a similar effect was observed in Cx43 null heart (median REV lower by 53.3% than that of the wildtype heart [67]), but not in Cx43 null cultured cortical astrocytes [8], and both knockout and wildtype neonates were offspring of the same heterozygous mothers, we hypothesize that the REV reduction represents a compensatory effect imposed by the structured organ that may be released in isolated cells.

Our analysis has shown the strong intercoordination of expression of other genes with that of Cx43. We found that most genes that are synergistically expressed with Cx43 in the wildtype were significantly down-regulated the in brains of Cx43 null or heterozygous mice and that most of those antagonistically expressed with Cx43 in the wildtype were up-regulated in the Cx43 null or heterozygous brains. This observation is consistent with our previous studies on Cx43 null heart [67] and with the fact that the type of regulation for genes expressed in Cx43 null specimens (heart, cortical

astrocytes) is similar/opposite for most of the synergistically/antagonistically expressed genes in the wildtype specimens [8,67]. In addition, we observed a tendency for overall gene expression stability to be increased in the K43 brains for synergistically expressed genes with Cx43 in W brains and to be decreased for the antagonistically expressed ones. These findings strongly indicate that the effects on gene expression are not simply the result of replacing the coding region of Cx43 [33] or of Cx32 [47] with the promoterless *neo*^{r} gene.

Although studies are still underway to elucidate the mechanisms involved in the connexin regulation of the brain transcriptome, our findings of high expression coordination of Cx43 with other genes in the wildtype brain, the remarkable predictability of the regulation type in K43 from the coordination in wildtype brain, and the similarities and dissimilarities between K43 and K32 suggest that both Cx43 and Cx32 may act as central nodes in the brain transcriptome. As such transcriptomic nodes, connexin genes regulate the expression level, stability, and coordination of both unique and shared downstream genes.

Acknowledgements

The research was partially supported by NIH grants: DK41918, NS41282, MH65495.

Appendix A. Supplementary data

Supplementary data associated with this article can be found, in the online version, at doi:10.1016/j.bbamem.2004.12.002.

References

[1] K. Willecke, J. Eiberger, J.J. Degen, D. Eckardt, A. Romualdi, M. Guldenagel, U. Deutsch, G. Sohl, Structural and functional diversity of connexin genes in the mouse and human genome, Biol. Chem. 383 (2002) 725–737.

[2] S.G. Hormuzdi, M.A. Filippov, G. Mitropoulow, H. Monyer, R. Bruzzone, Electrical synapses: a dynamic signaling system that shapes the activity of neuronal networks, Biochim. Biophys. Acta 1662 (2004) 113–137.

[3] T. Nakase, C.C. Naus, Gap junctions and neurological disorders of the central nervous system, Biochim. Biophys. Acta 1662 (2004) 149–158.

[4] R. Dermietzel, Diversification of gap junction proteins (connexins) in the central nervous system and the concept of functional compartments, Cell Biol. Int. 22 (1998) 719–730.

[5] B.W. Connors, M.A. Long, Electrical synapses in the Mammalian brain, Annu. Rev. Neurosci. 27 (2004) 393–418.

[6] M.V. Bennett, R.S. Zukin, Electrical coupling and neuronal synchronization in the Mammalian brain, Neuron 41 (2004) 495–511;
M.V. Bennett, R.S. Zukin, Electrical coupling and neuronal synchronization in the Mammalian brain, Euron 41 (2004) 495–511.

[7] E. Scemes, D.C. Spray, The astrocytic syncytium, in: L. Herz (Ed.), Non-neuronal Cells of the Nervous System: Function and Dysfunction, Adv. Cell Molec. Biol., vol. 31, Elsevier, 2004, pp. 165–179.

[8] D.A. Iacobas, M. Urban-Maldonado, S. Iacobas, E. Scemes, D.C. Spray, Array analysis of gene expression in connexin-43 null astrocytes, Physiol. Genomics 15 (3) (2003) 177–190.

[9] D.A. Iacobas, E. Scemes, D.C. Spray, Gene expression alteration in connexin43 null astrocytes extend beyond the gap junction, Neurochem. Int. 45 (2–3) (2004) 243–250.

[10] N.M. Kumar, N.B. Gilula, Cloning and characterization of human and rat liver cDNAs coding for a gap junction protein, J. Cell Biol. 103 (1986) 767–776.

[11] D.L. Paul, Molecular cloning of cDNA for rat liver gap junction protein, J. Cell Biol. 103 (1986) 123–134.

[12] R. Dermietzel, M. Farooq, J.A. Kessler, H. Althaus, E.L. Hertzberg, D.C. Spray, Oligodendrocytes express gap junction proteins connexin32 and connexin45, Glia 20 (2) (1997) 101–114.

[13] S.S. Scherer, S.M. Deschenes, Y.T. Xu, J.B. Grinspan, K.H. Fischbeck, D.L. Paul, Connexin32 is a myelin-related protein in the PNS and CNS, J. Neurosci. 15 (1995) 8281–8294.

[14] J. Bergoffen, S.S. Scherer, S. Wang, M.O. Scott, L.J. Bone, D.L. Paul, K. Chen, M.W. Lensch, P.F. Chance, K.H. Fischbeck, Connexin mutations in X-linked Charcot-Marie-Tooth disease, Science 262 (1993) 2039–2042.

[15] D.C. Spray, R. Dermietzel, X-linked dominant Charcot-Marie-Tooth disease and other potential gap-junction diseases of the nervous system, Trends Neurosci. 18 (6) (1995) 256–262.

[16] D.C. Spray, E. Scemes, R. Rozental, R. Dermietzel, Cell to cell signaling: an overview emphasizing gap junctions, in: J.H. Byrne, J.L. Roberts (Eds.), From Molecules to Networks: An Introduction to Cellular and Molecular Neuroscience, Academic Press, 2004, pp. 431–458.

[17] S.S. Scherer, Y.T. Xu, E. Nelles, K. Fischbeck, K. Willecke, L.J. Bone, Connexin32-null mice develop demyelinating peripheral neuropathy, Glia 24 (1998) 8–20.

[18] M.G. Hopperstad, M. Srinivas, A. Fort, D.C. Spray, Gap junction mutations in human disease, in: R.A. Maue (Ed.), Molecular and Cellular Insights to Ionic Channel Biology, Adv. Mol. Cell. Biol., vol. 32, 2004, pp. 161–187.

[19] K.H. Fischbeck, S.M. Deschenes, L.J. Bone, S.S. Scherer, Connexin32 and X-linked Charcot-Marie-Tooth disease, Cold Spring Harbor Symp. Quant. Biol. 61 (1996) 673–677.

[20] M.G. Lee, I. Nelson, H. Houlden, M.G. Sweeney, D. Hilton-Jones, J. Blake, N.W. Wood, M.M. Reilly, Six novel connexin32 (Gjb1) mutations in X-linked Charcot-Marie-Tooth disease, J. Neurol. Neurosurg. Psychiatry 73 (2002) 304–306.

[21] E.C. Beyer, D.L. Paul, D.A. Goodenough, Connexin43: a protein from rat heart homologous to a gap junction protein from liver, J. Cell Biol. 105 (1987) 2621–2629.

[22] Z.Q. Chen, D. Lefebvre, X.H. Bai, A. Reaume, J. Rossant, S.J. Lye, Identification of two regulatory elements within the promoter region of the mouse connexin 43 gene, J. Biol. Chem. 270 (1995) 3863–3868.

[23] D.C. Spray, T. Kojima, E. Scemes, S.O. Suadicani, Y. Gao, S. Zhao, A. Fort, "Negative" physiology: what connexin-deficient mice reveal about the functional role of individual gap junction proteins, Current Topics in Membranes, vol. 49, Academic Press, 2000, pp. 509–533.

[24] R. Dermietzel, O. Traub, T.K. Hwang, E. Beyer, M.V. Bennett, D.C. Spray, K. Willecke, Differential expression of three gap junction proteins in developing and mature brain tissues, Proc. Natl. Acad. Sci. U. S. A. 86 (24) (1989 (December)) 10148–10152.

[25] R. Dermietzel, E.L. Hertzberg, J.A. Kessler, D.C. Spray, Gap junctions between cultured astrocytes: immunocytochemical, molecular, and electrophysiological analysis, J. Neurosci. 11 (1991) 1421–1432.

[26] J.E. Rash, T. Yasumura, F.E. Dudek, J.I. Nagy, Cell-specific expression of conenxins and evidence of restricted gap junctional

coupling between glial cells and between neurons, J. Neurosci. 21 (2001) 1983–2000.
[27] E. Scemes, S.O. Suadicani, D.C. Spray, Intercellular communication in spinal cord astrocytes: fine tuning between gap junctions and P2 nucleotide receptors in calcium wave propagation, J. Neurosci. 20 (2000) 1435–1445.
[28] E.A. Bushong, M.E. Martone, Y.Z. Jones, M.H. Ellisman, Protoplasmic astrocytes in CA1 stratum radiatum occupy separate anatomical domains, J. Neurosci. 1;22 (1) (2002) 183–192.
[29] J.R. Wolff, K. Stuke, M. Missler, H. Trytko, P. Schwarz, A. Rohlmann, T.I. Chao, Autocellular coupling by gap junctions in cultured astrocytes: a new view on cellular autoregulation during process formation, Glia 24 (1998) 121–140.
[30] R. Rozental, M. Morales, M.F. Mehler, M. Urban, M. Kremer, R. Dermietzel, J.A. Kessler, D.C. Spray, Changes in the properties of gap junctions during neuronal differentiation of hippocampal progenitor cells, J. Neurosci. 18 (1998) 1753–1762.
[31] R. Rozental, M. Srinivas, S. Gokhan, M. Urban, R. Dermietzel, J.A. Kessler, D.C. Spray, M.F. Meltzer, Temporal expression of neuronal connexins during hippocampal ontogeny, Brain Res. Rev. 32 (2000) 57–71.
[32] N. Duval, D. Gomes, V. Calaora, A. Calabrese, P. Meda, R. Bruzzone, Cell coupling and Cx43 expression in embryonic mouse neural progenitor cells, J. Cell Sci. 115 (Pt 16) (2002) 3241–3251.
[33] A.G. Reaume, P.A. de Sousa, S. Kulkarni, B.L. Langille, D. Zhu, T.C. Davies, S.C. Juneja, G.M. Kidder, J. Rossant, Cardiac malformation in neonatal mice lacking connexin43, Science 267 (1995) 1831–1834.
[34] R. Dermietzel, Y. Gao, E. Scemes, D. Vieira, M. Urban, M. Kremer, M.V.L. Bennett, D.C. Spray, Connexin43 null mice reveal that astrocytes express multiple connexins, Brain Res. Rev. 32 (2000) 45–56.
[35] S. Fushiki, J.L. Perez Velazquez, L. Zhang, J.F. Bechberger, P.L. Carlen, C.C. Naus, Changes in neuronal migration in neocortex of connexin43 null mutant mice, J. Neuropathol. Exp. Neurol. 62 (3) (2003) 304–314.
[36] C. Lock, G. Hermans, R. Pedotti, A. Brendolan, E. Schadt, H. Garren, A. Langer-Gould, S. Strober, B. Cannella, J. Allard, P. Klonowski, A. Austin, N. Lad, N. Kaminski, S.J. Galli, J.R. Oksenberg, C.S. Raine, R. Heller, L. Steinman, Gene-microarray analysis of multiple sclerosis lesions yields new targets validated in autoimmune encephalomyelitis, Nat. Med. 8 (2002) 500–508.
[37] J.F. Loring, X. Wen, J.M. Lee, J. Seilhamer, R. Somogyi, A gene expression profile of Alzheimer's disease, DNA Cell Biol. 20 (2001) 683–695.
[38] S. Fushiki, J.L. Perez Velazquez, L. Zhang, J.F. Bechberger, P.L. Carlen, C.C. Naus, Changes in neuronal migration in neocortex of connexin43 null mutant mice, J. Neuropathol. Exp. Neurol. 62 (3) (2003) 304–314.
[39] D.H. Gutmann, N.M. Hedrick, J. Li, R. Nagarajan, A. Perry, M.A. Watson, Comparative gene expression profile analysis of neurofibromatosis 1-associated and sporadic pilocytic astrocytomas, Cancer Res. 1;62 (7) (2002) 2085–2091.
[40] E. Aronica, J.A. Gorter, G.H. Jansen, S. Leenstra, B. Yankaya, D. Troost, Expression of connexin 43 and connexin 32 gap-junction proteins in epilepsy-associated brain tumors and in the perilesional epileptic cortex, Acta Neuropathol. (Berl.) 101 (5) (2001) 449–459.
[41] E. Nelles, C. Butzler, D. Jung, A. Temme, H.D. Gabriel, U. Dahl, R. Dermietzel, K. Willecke, Defective propagation of signals generated by sympathetic nerve stimulation in the liver of connexin32-deficient mice, Proc. Natl. Acad. Sci. U. S. A. 93 (1996) 9565–9570.
[42] M.J. Vink, S.O. Suadicani, D.M. Vieira, M. Urban-Maldonado, Y. Gao, G.I. Fishman, D.C. Spray, Alterations of intercellular communication in neonatal cardiac myocytes from connexin43 null mice, Cardiovasc. Res. 62 (2) (2004) 397–406.
[43] D.A. Iacobas, M. Urban, A. Massimi, D.C. Spray, Improved procedure to mine the spotted cDNA arrays, J. Biomol. Tech. 13 (1) (2002) 5–19.
[44] D.A. Iacobas, M. Urban, A. Massimi, S. Iacobas, D.C. Spray, Hits and misses from gene expression ratio measurements in cDNA microarray studies, J. Biomol. Tech. 13 (3) (2002) 143–157.
[45] G.A. Churchill, Fundamentals of experimental design for cDNA microarrays, Nat. Genet. 32 Suppl. (2002) 490–495 (Review).
[46] A.J. Holloway, R.K. van Laar, R.W. Tothill, D.D. Bowtell, Options available from start to finish for obtaining data from DNA microarrays II, Nat. Genet. 32 Suppl. (2002) 481–489.
[47] M.K. Kerr, G.A. Churchill, Statistical design and the analysis of gene expression microarrays, Genet. Res. 77 (2001) 123–128.
[48] T.J. Belbin, J. Gaspar, M. Haigentz, R. Perez-Soler, S.M. Keller, M.B. Prystowsky, G. Childs, N.D. Socci, Indirect measurements of differential gene expression with cDNA microarrays, Biotechniques 36 (2004) 310–314.
[49] B. Merriman, A comparison of multiple microarray platforms for gene expression, ABRF Annual Meeting, RT5, 2004.
[50] D.A. Iacobas, Medical biostatistics, 3rd Eng Ed., Bucura Mond, Bucharest, 1997.
[51] D. Stekel, Microarray bioinformatics, Cambridge University Press, Cambridge, 2003.
[52] S. Draghici, Data analysis tools for DNA microarrays, Chapman & Hall, CRC Boca Raton, London, New York, Washington DC, 2003.
[53] D.A. Iacobas, Exploring the gene expression, in: D.A. Iacobas (Ed.), Ideas and Methods in the Physics of Living, 4th English ed., Tilia Press Intl., Constanta, 2000, pp. 273–305.
[54] D.A. Iacobas, S. Iacobas, D.C. Spray, The "patholog" of the genes expression profile, a new tool in defining, evaluating, and classifying the genetic diseases, Rom. J. Physiol. 37 (2000) 59–67.
[55] T. Nakase, G. Sohl, M. Theis, K. Willecke, C.C. Naus, Increased apoptosis and inflammation after focal brain ischemia in mice lacking connexin43 in astrocytes, Am. J. Pathol. 164 (2004) 2067–2075.
[56] M. Theis, R. Jauch, L. Zhuo, D. Speidel, A. Wallraff, B. Doring, C. Frisch, G. Sohl, B. Teubner, C. Euwens, J. Huston, C. Steinhauser, A. Messing, U. Heinemann, K. Willecke, Accelerated hippocampal spreading depression and enhanced locomotory activity in mice with astrocyte-directed inactivation of connexin43, J. Neurosci. 23 (2003) 766–776.
[57] W.A. Paznekas, S.A. Boyadjiev, R.E. Shapiro, O. Daniels, B. Wollnik, C.E. Keegan, J.W. Innis, M.B. Dinulos, C. Christian, M.C. Hannibal, E.W. Jabs, Connexin43 (GJA1) mutations cause the pleiotropic phenotype oculodentodigital dysplasia, Am. J. Hum. Genet. 72 (2003) 408–418.
[58] K. Oguro, T. Jover, H. Tanaka, Y. Lin, T. Kojima, N. Oguro, S.Y. Grooms, M.V. Bennett, R.S. Zukin, Global ischemia-induced increases in the gap junctional protein connexin 32 (Cx32) and Cx36 in hippocampus and enhanced vulnerability of Cx32 knock-out mice, J. Neurosci. 21 (2001) 7534–7542.
[59] B. Sutor, C. Schmolke, B. Teubner, C. Schirmer, K. Willecke, Myelination defects and neuronal hyperexcitability in the neocortex of connexin 32-deficient mice, Cereb. Cortex 10 (2000) 684–697.
[60] K.A. Kleopa, S.W. Yum, S.S. Scherer, Cellular mechanisms of connexin32 mutations associated with CNS manifestations, J. Neurosci. Res. 68 (5) (2002) 522–534.
[61] C.O. Hanemann, C. Bergmann, J. Senderek, K. Zerres, A.D. Sperfeld, Transient, recurrent, white matter lesions in X-linked Charcot-Marie-Tooth disease with novel connexin 32 mutation, Arch. Neurol. 60 (2003) 605–609.
[62] H.L. Paulson, J.Y. Barbern, T.F. Hoban, K.M. Krajewski, R.A. Lewis, K.H. Fischbeck, R.I. Grossman, R. Lenkinski, J.A. Kamholz, M.E. Shy, Transient central nervous system white matter abnormality in X-linked Charcot-Marie-Tooth disease, Ann. Neurol. 52 (2002) 429–434.
[63] P. Seeman, R. Mazanec, M. Ctvrteckova, D. Smikova, Charcot-Marie-Tooth type X. A novel mutation in the Cx32 gene with central conduction slowing, Int. J. Mol. Med. 8 (2001) 461–468.

[64] M. Bahr, F. Andres, V. Timmerman, M.E. Nelis, C. Van Broeckhoven, J. Dichgans, Central visual, acoustic, and motor pathway involvement in a Charcot-Marie-Tooth family with an Asn205Ser mutation in the connexin 32 gene, J. Neurol. Neurosurg. Psychiatry 66 (1999) 202–206.
[65] H. Takashima, M. Nakagawa, F. Umehara, K. Hirata, M. Suehara, H. Mayum, K. Yoshishige, W. Matsuyama, M. Saito, M. Jonosono, K. Arimura, M. Osa, Gap junction protein beta 1 (GJB1) mutations and central nervous system symptoms in X-linked Charcot-Marie-Tooth disease, Acta Neurol. Scand. 107 (2003) 31–37.
[66] A. Plum, G. Hallas, T. Magin, F. Dombrowski, A. Hagendorff, B. Schumacher, C. Wolpert, J. Kim, W.H. Lamers, M. Evert, P. Meda, O. Traub, K. Willecke, Unique and shared functions of different connexins in mice, Curr. Biol. 10 (1083) (2000) 1091.
[67] D.A. Iacobas, S. Iacobas, D.C. Spray, Use of cDNA arrays to explore gene expression in genetically manipulated mice and cell lines, in: S. Dhein, F.W. Mohr, M. Delmar (Eds.), In "Practical Methods in Cardiovascular Research", Springer-Verlag, 2005, pp. 887–895. ISBN: 3-540-40763-4.